

Metallacycles

Metallapentalenofuran: Shifting Metallafuran Rings Promoted by Substituent Effects

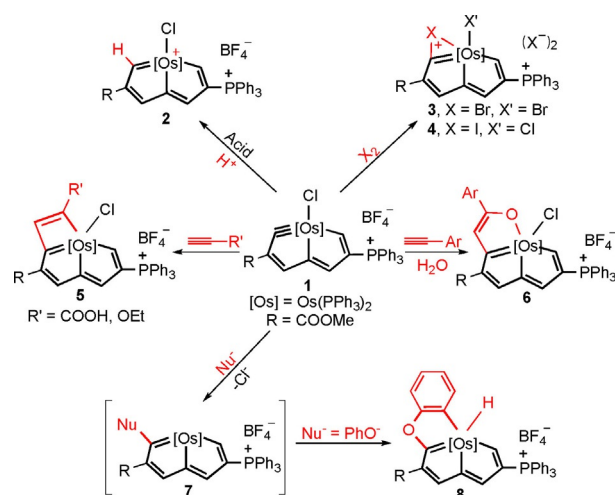
Yuhui Hua^{+, [a]}, Qing Lan^{+, [a]}, Jiawei Fei^{, [a]}, Chun Tang^{, [a]}, Jianfeng Lin^{, [a]}, Hexukun Zha^{, [a]},
Shiyan Chen^{, [a]}, Yinghua Lu^{, [a]}, Jiangxi Chen^{, * [b]}, Xumin He^{, * [a]} and Haiping Xia^{, [a]}

Abstract: Bulky substituents play important roles in controlling the reaction pathways or producing selected products. This work reports that the shift of metallafuran rings in a metallapentalenofuran complex can be promoted by the substituent effect via a reversible C–H bond reductive elimination and oxidative addition. The starting osmapentalyne, a so-called 7-carbon carbolong complex, was produced by the

oxidation of a metallapentalenofuran with FeCl₃. It was then allowed to react with nucleophiles, followed by a C–H activation, to give the aforementioned metallapentalenofuran complex. This work enriches the family of carbolong complexes and reveals a new strategy to promote, but not prevent reactions by the bulky substituents.

Introduction

Conjugated metallacycles, such as metallabenzenes,^[1,2] metallabenzynes,^[3,4] metallaannulenes,^[5] or others,^[6] are very interesting organometallic complexes due to their highly conjugated frameworks. Such frameworks should provide them with excellent stability, because they may exhibit Hückel^[7] or Möbius^[8] aromaticity. Recently, metallacycles with spiro-aromaticity^[9] have also been reported. As the first Craig-type Möbius metallacycle,^[10] osmapentalyne (**1**, Scheme 1) is a 7-carbon “carbolong complex”^[11] with novel reactivity and unique properties. For example, osmapentalyne **1** can undergo an electrophilic addition reaction with H⁺ to give the 16e osmapentalene (**2**),^[12] or with X₂ to give complexes **3** and **4**.^[13] The cycloaddition of complex **1** with terminal alkynes in the absence or presence of water can occur to give cycloaddition products such as cyclobutametallapentalenes (**5**)^[14] or α-metallapentalenofurans (**6**),^[15] respectively. It is interesting to note that osmapentalyne **1** can also react with nucleophiles^[16] (e.g., alkoxides) to give



Scheme 1. Chemical reactivity of osmapentalyne **1**.

addition products. This reaction is followed by a C–H oxidative addition to give β-metallapentalenofurans (**8**), when the nucleophile was an aryloxy anion (Scheme 1).^[17]

Unlike most reported carbolong complexes, in which the metallacyclic frameworks are composed of a metal and carbon atoms, metallapentalenofurans are oxygen-containing metallacycles, and can be viewed as a Craig-type Möbius aromatics derived from 11-center-12-electron d_π-p_π π-conjugation. In our efforts to develop carbolong chemistry, we have reported that α-metallapentalenofuran (**6**) can show J-aggregates behavior and display photothermal properties.^[18] However, the chemistry of β-metallapentalenofurans (**8**) has still been under studied.^[19] In this work, we report the reverse of reductive elimination and oxidative addition between β-metallapentalenofurans and metallapentalynes, which enriches the reactivity of carbolong complexes. The reaction mechanism was also studied with the help of DFT calculations.

[a] Y. Hua,⁺ Q. Lan,⁺ J. Fei, C. Tang, J. Lin, H. Zha, S. Chen, Y. Lu, Prof. Dr. X. He, Prof. Dr. H. Xia
State Key Laboratory of Physical Chemistry of Solid Surfaces
and Collaborative Innovation Center of Chemistry for Energy Materials (iChEM)
College of Chemistry and Chemical Engineering
Xiamen University, Xiamen 361005 (China)
E-mail: hejin@xmu.edu.cn

[b] Dr. J. Chen
Department of Materials Science and Engineering
College of Materials, Xiamen University
Xiamen 361005 (China)
E-mail: chenjx@xmu.edu.cn

[*] These authors contributed equally to this work.

Supporting information and the ORCID identification number(s) for the author(s) of this article can be found under:
<https://doi.org/10.1002/chem.201802928>.

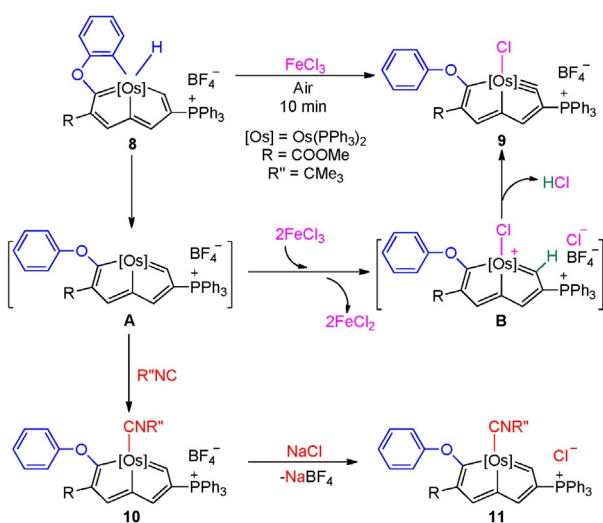
Results and Discussion

Synthesis of osmapentalynes

In our previous study, the nucleophilic attack of the cyclic metal carbyne of osmapentalyne **1** followed by a C–H bond oxidative addition led to a complex **8**, which was isolated in 47% yield, when the nucleophile was the PhO[−] generated in situ from PhOH in the presence of Cs₂CO₃ at room temperature.^[17]

Treatment of osmapentalenofuran **8** with FeCl₃ in air quickly produced osmapentalyne **9**, the structure of which was assigned on the basis of NMR and HRMS data. The ³¹P{¹H} NMR spectrum of the complex **9** shows two resonances at δ = 4.85 (t, J_{P,P} = 5.0 Hz, CPh₃) and 1.14 ppm (d, J_{P,P} = 5.0 Hz, OsPPh₃), which are similar to those reported for osmapentalynes.^[16a] In the ¹³C{¹H} NMR spectrum of **9**, the peak corresponding to the metal–carbyne (C1) was located at δ = 328.8 ppm. The other signals of carbon atoms in the metallacycle appear at δ = 135.4, 151.4, 173.6, 160.2, 144.2, and 246.1 ppm for C2, C3, C4, C5, C6, and C7, respectively. For comparison, signals from the reported osmapentalynes^[16a] were observed at δ = 324.5, 119.1, 158.5, 182.0, 154.3, 155.6, and 227.9 ppm for C1, C2, C3, C4, C5, C6, and C7, respectively. The ¹H NMR spectrum of the complex **9** shows the signals for the metallacyclic protons at δ = 7.46 (H3) and 8.68 ppm (H5). These values are also similar to those from the reported osmapentalyne, indicating that complex **9** has a similar metallacyclic structure. The molecular formula of complex **9** was further confirmed by HRMS (*m/z* : 1251.2598, Figure S6, Supporting Information) data.

As shown in Scheme 2, a mechanism for the formation of complex **9** is proposed as follows: at first, the reductive elimination of **8** occurs to give the 16e osmapentalene intermediate (**A**), which is subsequently oxidized by FeCl₃ to give the higher valent chloro-osmapentalene intermediate (**B**). Then, the known deprotonation^[12] of the intermediate **B** gives the osmapentalyne **9** as the final product.



Scheme 2. Proposed mechanism for the formation of **9** from **8** and the isolation of **10** and **11**.

The presence of the 16e osmapentalene intermediate **A** is strongly supported by the isolation of a complex (**10**) from the reaction of complex **8** with *tert*-butylisocyanide. The structure of **10** was confirmed by NMR spectroscopy, HRMS data (Figures S7–S13), and elemental analysis. In the ¹H NMR spectrum, the resonance of the H1 proton is located at δ = 11.91 ppm (d, J_{P,H} = 22.0 Hz), which is similar to the spectra of reported osmapentalenes (δ = 11.83–14.96 ppm).^[10c] The signals of other protons in the fused rings are observed in the aromatic region (δ = 7.00–8.70 ppm). In the ³¹P{¹H} NMR spectrum, the CPh₃ signal appears at 11.00 ppm, and the two OsPPh₃ signals appear at δ = 6.67 ppm. The ¹³C{¹H} NMR spectrum of complex **10** displays the signals in the downfield region at δ = 244.6 (s, C7), 2145 (s, C1), and 197.0 ppm (d, J_{P,C} = 27.6 Hz, C4) for carbon atoms bonded to metal; the other signals for carbon atoms in metallacycles appeared at δ = 134.7, 150.4 (d, J_{P,C} = 25.9 Hz), 161.9, and 155.7 ppm for C2, C3, C5, and C6, respectively. However, we were unable to grow single crystals of complex **10**. To further confirm the metallacyclic structure of **10** and the occurrence of the reductive elimination of complex **8** in the presence of *tert*-butylisocyanide, we successfully acquired a high-quality single crystal of complex **11**, by an anion exchange reaction of **10** with NaCl (Scheme 2). As shown in Figure 1, **11** contains a near-planar metal-bridged bicyclic structure, as reflected by the small mean deviation from the least-squares plane (0.066 Å). The Os–C bond lengths of **11** (2.085 for Os1–C1, 2.072 for Os1–C4, and 2.023 Å for Os1–C7) are close to those for reported osmapentalenes (1.926–2.175 Å).^[10,12,14,17,18e] Complex **11** represents a new 18e osmapentalene, which strongly supports the existence of the 16e osmapentalene intermediate **A**.

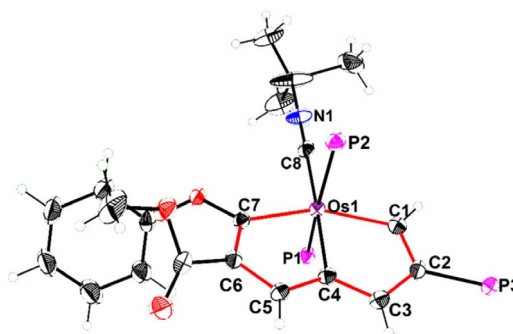
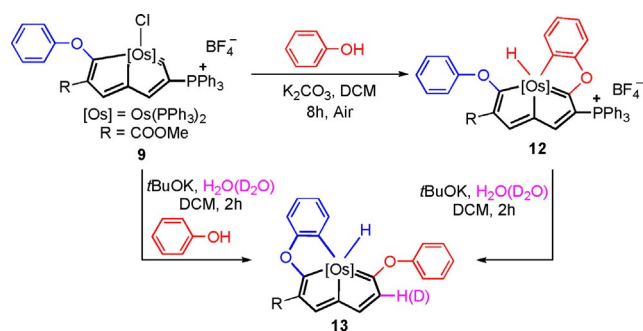


Figure 1. X-ray molecular structure of the cation of complex **11** drawn at the 50% probability level. Phenyl groups in PPh₃ moieties were omitted for clarity. Selected bond lengths [Å] and angles [°]: Os–C1: 2.085(5), Os1–C4: 2.072(5), Os1–C7: 2.023(5), Os1–C8: 1.987(5), C1–C2: 1.382(7), C2–C3: 1.431(7), C3–C4: 1.381(7), C4–C5: 1.422(7), C5–C6: 1.375(6), C6–C7: 1.454(6); Os1–C1–C2: 115.9(4), C1–C2–C3: 116.4(4), C2–C3–C4: 112.5(4), C3–C4–Os1: 118.6(3), C4–Os1–C1: 76.6(19), Os1–C4–C5: 115.6(3), C4–C5–C6: 114.9(4), C5–C6–C7: 114.2(4), C6–C7–Os1: 115.9(3), C7–Os1–C4: 77.9(19), P1–Os1–P2: 167.8(5).

Shiftable metallafuran rings

The formation of the osmapentalyne **9** motivated us to re-investigate the aforementioned nucleophilic reaction of osmapentalyne with phenol in the presence of base.^[17] As expected, treatment of osmapentalyne **9** with excess PhOH in the pres-



Scheme 3. Synthesis of **13** in one or two steps from complex **9**.

ence of K_2CO_3 in air produced the osmapentalenofuran **12** (Scheme 3).

The structure of **12** was confirmed by single-crystal X-ray diffraction analysis. As shown in Figure 2, the metallacyclic unit in **12** (Comprised of Os1, O1, and C1–C9) is almost planar, as reflected by the small mean deviation from the least-squares plane (0.052 Å). It can be noted that **12** was the first β -metallapentalenofuran characterized by single-crystal X-ray crystallography, despite the fact that the β -metallapentalenofuran **8** was reported in an early primary communication.^[17] The interesting structural feature of **12** is the presence of a phenoxy group on the metallacycle.

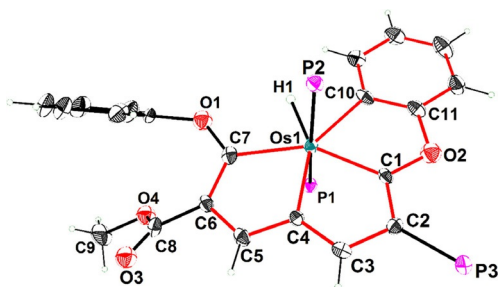


Figure 2. X-ray molecular structure for the cation of complex **12** drawn with a 50% probability level. The phenyl groups in PPh_3 moieties are omitted for clarity. Selected bond lengths [Å] and angles [°]: Os–C1: 2.054(3), Os1–C4: 2.096(3), Os1–C7: 2.084(3), Os1–C11: 2.152(3), C1–C2: 1.401(4), C2–C3: 1.408(4), C3–C4: 1.388(4), C4–C5: 1.400(4), C5–C6: 1.381(4), C6–C7: 1.415(4), C10–C11: 1.395(4), C11–O2: 1.385(4), C1–O2: 1.350(3); Os1–C1–C2: 120.9(2), C1–C2–C3: 111.5(3), C2–C3–C4: 115.2(4), C3–C4–Os1: 117.9(2), C4–Os1–C1: 74.52(12), Os1–C4–C5: 118.1(2), C4–C5–C6: 114.8(3), C5–C6–C7: 113.1(3), C6–C7–Os1: 118.6(2), C7–Os1–C4: 74.38(12), Os1–C10–C11: 114.2(2), C10–C11–O2: 117.1(3), C11–O2–C1: 112.3(2), O2–C1–Os1: 122.2(2), C1–Os1–C10: 74.0(11), P1–Os1–P2: 175.69(2).

The molecular structure of **12** was further confirmed by multinuclear NMR. In the 1H NMR (Figure S20, Supporting Information), the signals of H3, H5, and Os–H are at $\delta = 8.80$, 8.76, and -2.32 ppm, respectively, which are similar to those of the complex **8**. In the $^{31}P\{^1H\}$ NMR (Figure S21, Supporting Information), the CPh_3 signal appears at $\delta = 8.29$ ppm, and two $OsPPh_3$ signals appear at $\delta = -2.26$ ppm. In the $^{13}C\{^1H\}$ NMR (Figure S22, Supporting Information), the signals of C1, C4, and C7 and C10 are located at $\delta = 249.4$ (dd, $J_{P-C} = 13.6$, $J_{P-C} = 6.2$ Hz), 184.3 (dt, $J_{P-C} = 27.3$, $J_{P-C} = 3.2$ Hz), and 169.1 ppm (br), respectively. The

molecular formula of **12** was also confirmed by HRMS (m/z : 1309.3349, Figure S25, Supporting Information) data.

Surprisingly, the reaction of **12** with $tBuOK$ eliminated the phosphonium group attached at C2 and produced **13** in the presence of H_2O . Obviously, the metallafuran ring shifted from the right (Scheme 3, **12**) to the left (**13**) through the reversible reductive elimination and oxidative addition of Ar–H bond on the metal center.

The molecular structure of the **13** was also confirmed by single-crystal X-ray diffraction analysis. As shown in Figure 3, **13** has a metallacyclic structure similar to that of **12**, except that it contains different substituents on the metallacycle. The

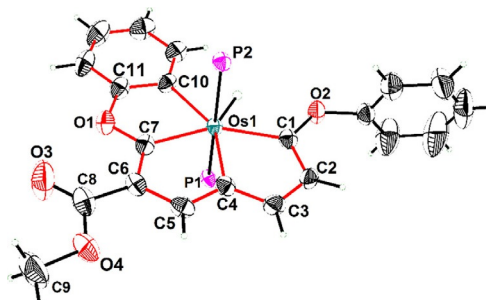


Figure 3. The X-ray molecular structure for the complex **13** drawn with 50% probability level. The phenyl groups in PPh_3 moieties are omitted for clarity. Selected bond lengths [Å] and angles [°]: Os–C1: 2.081(3), Os1–C4: 2.109(2), Os1–C7: 2.060(3), Os1–C10: 2.142(2), C1–C2: 1.399(4), C2–C3: 1.389(4), C3–C4: 1.387(4), C4–C5: 1.385(4), C5–C6: 1.394(4), C6–C7: 1.419(4), C7–O1: 1.352(3), O1–C11: 1.391(3), C11–C10: 1.387(4), Os1–C1–C2: 119.83(19), C1–C2–C3: 112.9(3), C2–C3–C4: 115.0(2), C3–C4–Os1: 118.14(19), C4–Os1–C1: 73.91(10), Os1–C4–C5: 117.8(2), C4–C5–C6: 115.8(2), C5–C6–C7: 111.5(2), C6–C7–Os1: 120.6(2), C7–Os1–C4: 74.31(10), Os1–C10–C11: 114.73(19), C10–C11–O1: 117.2(2), C11–O1–C7: 111.8(2), O1–C7–Os1: 122.12(18), C7–Os1–C10: 73.99(10), P1–Os1–P2: 174.51(2).

molecular structure of **13** was further confirmed by multinuclear NMR and elemental analysis, as well as HRMS (Figures S26–S31, Supporting Information) data. In particular, the hydride signal of **13** in the 1H NMR (Figure S26, Supporting Information) appears at $\delta = -3.11$ ppm, which is similar to those for **8** and **12**. In the $^{31}P\{^1H\}$ NMR spectrum (Figure S27, Supporting Information), the signal at $\delta = -0.23$ ppm is assigned for the two $OsPPh_3$ groups.

Despite the fact that K_2CO_3 is a weaker base than $tBuOK$, both of them are strong enough to take away the acidic proton of PhOH to generate PhO^- , which acted as a nucleophile to attack the osmapentalene **9**. However, only the stronger base ($tBuOK$) can eliminate the phosphonium group of PPh_3 , resulting in the shift of the metallafuran ring through the reversible reductive elimination and oxidative addition of the Ar–H bond on the metal center. It is noted that the base has also been found to play an important role in transition-metal-catalyzed organic reactions.^[20] When D_2O was used in this phosphonium-eliminated reaction, the deuterium-labeled complex **13D** was isolated and its structure was supported by 2D NMR (Figure S33, Supporting Information) and HRMS (m/z : 1072.2471, Figure S34, Supporting Information) data, which in-

indicated that the proton attached at C2 was originated from water.

DFT studies

The interesting behavior of the metallafuran ring in the reversible reductive elimination and oxidative addition of the Ar–H bond on the osmium in complexes **12** and **13** motivated us to investigate the origin of this shift. The DFT results indicate that the elimination of the phosphonium group in **12** to give intermediate **14** is thermodynamically favorable ($-192.3 \text{ kcal mol}^{-1}$, Figure 4). The reductive elimination of intermediate **14** occurs with a small barrier of $16.5 \text{ kcal mol}^{-1}$ to give the 16e osmapentalene intermediate **15**, which is similar to the intermediate **A** shown in Scheme 2. Then, the 16e osmapentalene intermediate **15** is converted to the thermodynamically stable complex **13** by the oxidative addition of the phenoxy group on the left side (Figure 4) with a very small barrier of $0.04 \text{ kcal mol}^{-1}$. In contrast, the shift of the metallafuran ring of **12** itself to give **16** (a hypothetical complex) was not observed in our experiments. The DFT result reveals that it is of thermodynamic origin: complex **12** is thermodynamically more favorable ($9.79 \text{ kcal mol}^{-1}$) than complex **16**.

To further understand the influence of substituents in the shift of the metallafuran ring, we calculated the Gibbs free energy profiles of a series of metallapentalenofurans with different substituents (Figure 5). When the substituent of $[\text{PPh}_3]^+$ was changed to $[\text{PH}_3]^+$, the resulting complex **20** is more thermodynamically unfavorable ($2.65 \text{ kcal mol}^{-1}$) than complex **17** (Figure 5). This result suggests that the substituent effect should be steric in origin, because the $[\text{PPh}_3]^+$ and $[\text{PH}_3]^+$ groups are both strong electron-withdrawing groups. As expected, when the substituent is CMe_3 (large electron-donating group), the resulting metallapentalenofuran **22** is thermodynamically more favorable ($5.78 \text{ kcal mol}^{-1}$) than the metallapentalenofuran **19** (Figure 5). The strong electron-withdrawing CF_3 group, which is slightly larger than the $[\text{PH}_3]^+$ group but smaller than the CMe_3 group, only shows a small energy difference

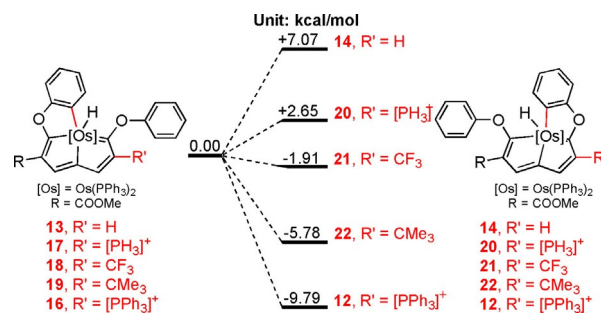


Figure 5. Gibbs free-energy profiles for the energy differences between two types of metallapentalenofurans calculated by DFT methods.

of $1.91 \text{ kcal mol}^{-1}$. Thus, the bigger substituent, the more stable is the structure on the right (Figure 5).

To understand how the steric effect works, we took a close look at the optimized structure of complexes **16** and **17**. As shown in Figure 6, when the substituent is a $[\text{PPh}_3]^+$ group, the structure of **16** has very short distances of H–H (2.22 \AA) and C–C (3.37 \AA), which are shorter than the sums of van der Waals radii of H–H (2.40 \AA) and C–C (3.40 \AA), respectively, suggesting the presence of strong repulsive interactions.^[21] Inter-

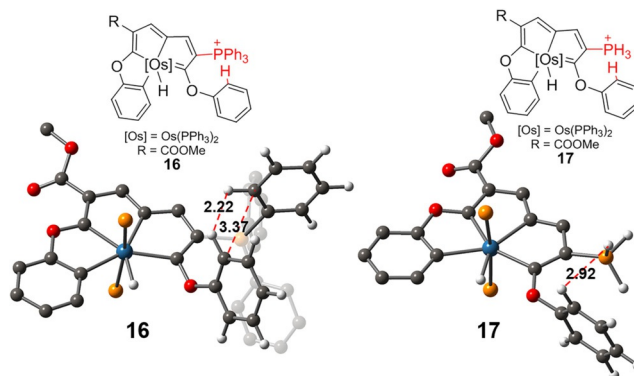


Figure 6. DFT-optimized structures of **16** and **17** with omitting partial hydrogen atoms and Ph groups for clarity.

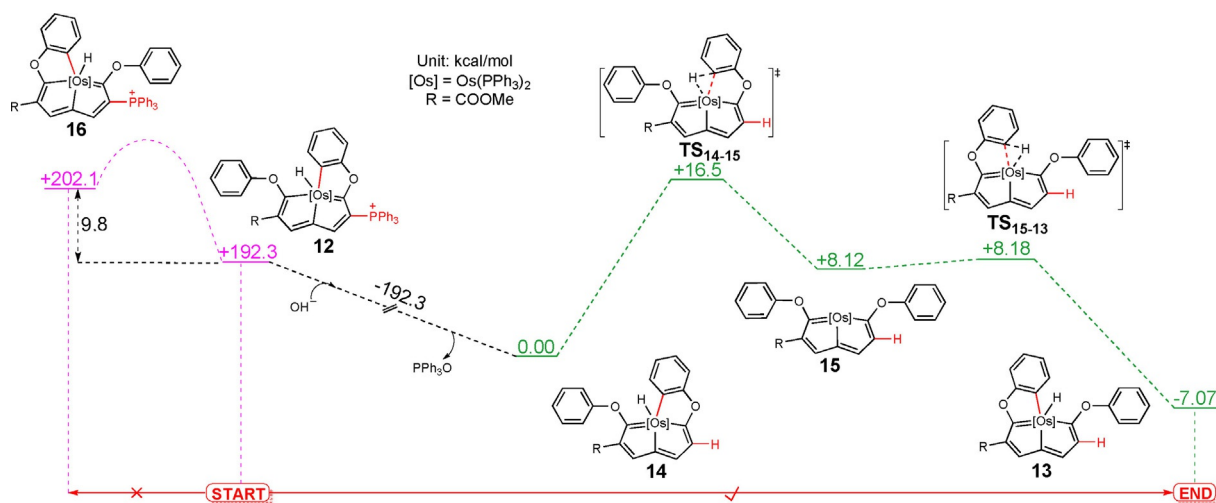


Figure 4. Gibbs free energy profiles for the possible mechanism of the formation of complex **13** from **12** calculated by DFT methods.

estingly, both short interactions disappeared after the formation of metallafuran ring in complex **12**, because the benzene ring changes its orientation and thus relieves the repulsion. When the substituent is the much smaller $[\text{PH}_3]^+$ group, the H–H distance in the resulting complex **17** is 2.92 Å. Thus, **17** does not experience any repulsion. These results explain why the steric effect dominated in these reactions.

Conclusions

In summary, a new approach for the synthesis of a 7-carbon osmium carbonyl complex was developed from the oxidation of an osmapentalenofuran with FeCl_3 in air via the 16e osmapentalene intermediate. This 7-carbon osmium carbonyl complex can further undergo a nucleophilic reaction with phenol in the presence of base. It is interesting to find that the metallafuran rings can shift in a manner that is dominated by the sizes of the substituents on the metallacycle. The results provide very interesting examples that enrich the carbonyl chemistry.

Experimental Section

General information

All the reactions were carried out under a nitrogen atmosphere using standard Schlenk techniques unless otherwise stated. Complexes **1**^[16a] and **8**^[17] was prepared by following the procedure in the literature. Other commercial reagents were used without further purification. NMR spectroscopic experiments were performed on a Bruker AVIII-400 (^1H , 400.1, ^{13}C , 100.6, ^{31}P , 162.0 MHz) spectrometer, a Bruker AVIII-500 (^1H , 500.2, ^{13}C , 125.8, ^{31}P , 202.5 MHz) spectrometer, or a Bruker Ascend III 600 (^1H , 600.1, ^{13}C , 150.9, ^{31}P , 242.9 MHz) spectrometer at room temperature. ^1H and ^{13}C NMR chemical shifts (δ) are relative to tetramethylsilane, and ^{31}P NMR chemical shifts are relative to 85% H_3PO_4 . The absolute values of the coupling constants are given in hertz. Multiplicities are abbreviated as singlet (s), doublet (d), triplet (t), multiplet (m), and broad (br). HRMS experiments were performed on a Bruker En Apex Ultra 7.0T FT-MS. Elemental analysis data were collected using a Vario EL III elemental analyzer.

Complex 9

A mixture of **8** (650 mg, 0.5 mmol) and FeCl_3 (400 mg, 2.5 mmol) in dichloromethane (20 mL) was stirred at room temperature for 10 min in air to give a yellow/brown solution. The solution was extracted with H_2O (3×30 mL), and the organic phase was collected. The orange solid of **9** (602 mg, yield: 90%) was collected after the solvent was evaporated to dryness under vacuum and the resulting residue was washed with diethyl ether and then dried under vacuum. ^1H NMR plus ^1H - ^{13}C HSQC (500.2 MHz, CD_2Cl_2): δ = 8.68 (s, 1H, H5), 7.46 (s, 1H, H3), 6.20 (d, $J_{\text{H-H}} = 8.7$ Hz, 2H, H11 H15), 2.98 ppm (s, 3H, COOMe); ^{31}P NMR (202.5 MHz, CD_2Cl_2): δ = 4.85 (t, $J_{\text{P-P}} = 5.0$ Hz, COPh_3), 1.14 ppm (d, $J_{\text{P-P}} = 5.00$ Hz Os(PPh_3)₂); ^{13}C NMR plus DEPT-135, ^1H - ^{13}C HSQC and ^1H - ^{13}C HMBC (125.8 MHz, CD_2Cl_2): δ = 328.8 (dd, $J_{\text{P-C}} = 13.6$, $J_{\text{P-C}} = 13.5$ Hz, C1), 246.1 (t, $J_{\text{P-C}} = 8.7$ Hz, C7), 173.6 (d, $J_{\text{P-C}} = 22.8$ Hz, C4), 163.6 (s, C8), 160.2 (s, C5), 159.8 (s, C10), 151.4 (d, $J_{\text{P-C}} = 15.4$ Hz, C3), 144.2 (s, C6), 135.4 (d, $J_{\text{P-C}} = 69.0$ Hz, C2), 116.5–135.1 (m, other aromatic carbons), 51.0 ppm (s, C9); HRMS (ESI): m/z : calcd for $[\text{C}_{69}\text{H}_{55}\text{ClO}_3\text{OsP}_3]^+$: 1251.2662;

found: 1251.2598; elemental analysis calcd (%) for $\text{C}_{69}\text{H}_{55}\text{BClF}_4\text{O}_3\text{OsP}_3$: C 61.96, H 4.14; found: C 62.10, H 4.34.

Complex 10

$t\text{BuNC}$ (113 μL , 1 mmol) was injected into a solution of **8** (130 mg, 0.1 mmol) in CH_2Cl_2 . The reaction mixture was stirred at room temperature for 3 days to give a yellow/green solution. The solution was evaporated under vacuum to a volume of approximately 2 mL and then purified by column chromatography (neutral alumina, eluent: dichloromethane/ methanol 20:1) to give a yellow/green solution. The yellow/green solid of **10** (90 mg, 65%) was collected after the solvent was evaporated to dryness under vacuum. ^1H NMR plus ^1H - ^{13}C HSQC (600.1 MHz, CD_2Cl_2): δ = 11.91 (d, $J_{\text{P-H}} = 22.0$ Hz, 1H, H1), 8.70 (s, 1H, H5), 8.55 (s, 1H, H3), 2.87 (s, 3H, H10), 0.89 ppm (s, 9H, $t\text{Bu}$); ^{31}P NMR: (242.9 MHz, CD_2Cl_2): δ = 11.00 (s, COPh_3), 6.67 ppm (s, Os(PPh_3)₂); ^{13}C NMR plus DEPT-135, ^1H - ^{13}C HSQC, and ^1H - ^{13}C HMBC (150.9 MHz, CD_2Cl_2): δ = 244.6 (s, C7), 214.5 (s, C1), 197.0 (d, $J_{\text{P-C}} = 27.6$ Hz, C4), 164.5 (s, C9), 161.9 (s, C5), 159.1 (s, C11), 155.7 (s, C6), 150.4 (d, $J_{\text{P-C}} = 25.9$ Hz, C3), 140.0 (m, C8), 134.7 (m, C2), 117.1–134.1 (m, other aromatic carbon atoms), 50.2 (s, C10), 55.8 (s, $t\text{Bu}$), 30.2 ppm (s, $t\text{Bu}$); HRMS (ESI): m/z : calcd for $[\text{C}_{74}\text{H}_{65}\text{NO}_3\text{OsP}_3]^+$: 1300.3787; found: 1300.3779; elemental analysis calcd (%) for $\text{C}_{74}\text{H}_{65}\text{BF}_4\text{NO}_3\text{OsP}_3$: C 64.11, H 4.73, N 1.01; found: C 64.53, H 5.12, N 1.34.

Complex 11

Excess NaCl was added into a solution of **10** (160 mg, 0.12 mmol) in CH_2Cl_2 . The reaction mixture was stirred at room temperature for 5 h to give a yellow/green solution. The solution was then purified by extraction with H_2O (3×10 mL), and the organic phase collected. The yellow-green solid of **11** (145 mg, 91%) was collected after the solvent was evaporated to dryness under vacuum. ^1H NMR plus ^1H - ^{13}C HSQC (400.1 MHz, CD_2Cl_2): δ = 11.92 (d, $J_{\text{P-H}} = 22.0$ Hz, 1H, H1), 8.70 (s, 1H, H5), 8.57 (s, 1H, H3), 2.88 (s, 3H, H10), 0.89 ppm (s, 9H, $t\text{Bu}$); ^{31}P NMR: (161.9 MHz, CD_2Cl_2): δ = 11.55 (s, COPh_3), 7.17 ppm (s, Os(PPh_3)₂); ^{13}C NMR plus DEPT-135, ^1H - ^{13}C HSQC, and ^1H - ^{13}C HMBC (100.6 MHz, CD_2Cl_2): δ = 244.5 (m, C7), 214.4 (m, C1), 197.0 (dt, $J_{\text{P-C}} = 26.1$, $J_{\text{P-C}} = 4.3$ Hz, C4), 164.5 (s, C9), 161.8 (s, C5), 159.0 (s, C11), 155.6 (s, C6), 150.4 (d, $J_{\text{P-C}} = 26.0$ Hz, C3), 140.0 (m, C8), 134.6 (m, C2), 117.1–134.1 (m, other aromatic carbon atoms), 50.1 (s, C10), 55.8 (s, $t\text{Bu}$), 30.2 ppm (s, $t\text{Bu}$); elemental analysis calcd (%) for $\text{C}_{74}\text{H}_{65}\text{ClNO}_3\text{OsP}_3$: C 66.58, H 4.91, N 1.05; found: C 66.18, H 4.87, N 1.00.

Complex 12

A mixture of **10** (670 mg, 0.5 mmol), K_2CO_3 (685 mg, 5 mmol), and phenol (280 mg, 3 mmol) in dichloromethane (20 mL) was stirred at room temperature for 8 h to give a fuchsia solution. The solution was evaporated under vacuum to a volume of approximately 2 mL and then purified by column chromatography (neutral alumina, eluent: dichloromethane/acetone = 5:1) to give a fuchsia solution. The fuchsia solid of **12** (502 mg, 72%) was collected after the solvent was evaporated to dryness under vacuum. ^1H NMR plus ^1H - ^{13}C HSQC (400.0 MHz, CD_2Cl_2): δ = 8.80 (s, 1H, H5), 8.76 (s, 1H, H3), 7.56 (d, $J_{\text{H-H}} = 6.0$ Hz, 1H, H11), 6.95 (t, $J_{\text{H-H}} = 6.6$ Hz, 1H, H12), 6.30 (t, $J_{\text{H-H}} = 6.8$ Hz, 1H, H13), 6.08 (d, $J_{\text{H-H}} = 7.5$ Hz, 2H, H17 H21), 5.91 (d, $J_{\text{H-H}} = 7.6$ Hz, 1H, H14), 2.77 (s, 3H, COOMe), –2.31 ppm (t, $J_{\text{P-H}} = 16.0$ Hz, 1H, Os-H); ^{31}P NMR (161.9 MHz, CD_2Cl_2): δ = 8.29 (s, COPh_3), –2.26 ppm (s, Os (PPh_3)₂); ^{13}C NMR plus DEPT-135, ^1H - ^{13}C HSQC and ^1H - ^{13}C HMBC (100.6 MHz, CD_2Cl_2): δ = 249.4 (dt, $J_{\text{P-C}} = 4.92$ Hz, $J_{\text{P-C}} = 6.50$ Hz, C1), 213.0 (t, $J_{\text{P-C}} = 11.3$ Hz, C7), 184.4 (dt, $J_{\text{P-C}} =$

27.7 Hz, $J_{p,c} = 2.5$ Hz, C4), 169.1 (s, C15), 163.9 (s, C8), 163.6 (d, $J_{p,c} = 16.0$ Hz, C3), 162.9 (s, C5), 159.3 (s, C16), 147.6 (s, C11), 146.2 (s, C6), 134.9 (t, $J_{p,c} = 10.1$ Hz, C10), 127.4–134.8 (m, other aromatic carbon atoms), 124.7 (s, C12), 123.4 (s, C19), 123.1 (s, C13), 120.8 (d, $J_{p,c} = 89.4$ Hz, CPh), 116.8 (s, C18 C20), 134.1 (dt, $J_{p,c} = 52.8$, $J_{p,c} = 4.50$ Hz, C2), 111.3 (s, C14), 50.3 ppm (s, C9); HRMS (ESI): m/z : calcd for $[C_{75}H_{60}O_4OsP_3]^+$: 1309.3314; found: 1309.3349; elemental analysis calcd (%) for $C_{75}H_{60}BF_4O_4OsP_3$: C 64.56, H 4.33; found: C 64.47, H 4.77.

Complex 13

A mixture of **12** (405 mg, 0.3 mmol) and tBuOK (168 mg, 1.5 mmol) in dichloromethane/water (10/0.1 mL) was stirred at room temperature for 10 h to give an orange solution. The solution was evaporated under vacuum to a volume of approximately 2 mL and then purified by column chromatography (neutral alumina, eluent: dichloromethane) to give an orange solution. The orange solid of **13** (283 mg, yield = 90%) was collected after the solvent was evaporated to dryness under vacuum. 1H NMR plus 1H - ^{13}C HSQC (400.0 MHz, $CDCl_3$): $\delta = 9.06$ (s, 1H, H5), 8.00 (s, 1H, H3), 7.72 (d, $J_{H-H} = 6.6$ Hz, 1H, H15), 6.56 (brs, 2H, H12, H14), 6.28 (t, $J_{H-H} = 6.3$ Hz, H13), 6.18 (d, $J_{H-H} = 7.08$ Hz, 2H, H17, H21), 5.62 (s, 1H, H2), 3.77 (s, 3H, COOMe), -3.11 ppm (t, $J_{p,H} = 15.6$ Hz, 1H, Os–H); ^{31}P NMR (161.9 MHz, $CDCl_3$): $\delta = -0.23$ ppm (s, Os(PPh_3) $_2$); ^{13}C NMR plus DEPT-135, 1H - ^{13}C HSQC and 1H - ^{13}C HMBC (100.6 MHz, $CDCl_3$): $\delta = 245.1$ (t, $J_{p,c} = 7.66$ Hz, C7), 228.5 (t, $J_{p,c} = 11.9$ Hz, C4), 183.6 (br, C1), 170.0 (s, C11), 163.7 (s, C8), 160.7 (s, C5), 157.9 (s, C16), 157.4 (s, C3), 136.4 (t, $J_{p,c} = 9.9$ Hz, C10), 136.0 (s, C2), 134.3 (s, C6), 126.8–134.7 (m, other aromatic carbon atoms), 124.5 (s, C19), 123.4 (s, C12), 121.9 (s, C13), 121.7 (s, C17 C21), 111.5 (s, C14), 50.6 ppm (s, C9); HRMS (ESI): m/z : calcd for $[C_{57}H_{46}O_4OsP_2Na]^+$: 1071.2378; found: 1071.2399; elemental analysis calcd (%) for $C_{57}H_{46}O_4OsP_2$: C 65.38, H 4.43; found: C 65.15, H 4.88.

X-ray crystallographic analysis

Single crystals suitable for X-ray diffraction were grown from dichloromethane solutions of **11** and **12** layered with hexane, and from a methanol solution of **13** layered with hexane. Single-crystal X-ray diffraction data were collected on an Oxford Gemini S Ultra CCD area detector for **11–13**, with a $Mo_{K\alpha}$ radiation ($\lambda = 0.71073$ Å). The data were corrected for absorption effects using the multi-scan technique. Using Olex2,^[22] the structures of **11–13** were solved with the ShelXT^[23] structure solution program using Intrinsic Phasing and refined with the ShelXL^[24] refinement package using least-squares minimization. All of the non-hydrogen atoms were refined anisotropically unless otherwise stated. The hydrogen atoms were placed at their idealized positions and refined using a riding model unless otherwise stated. The solvent CH_2Cl_2 and phenyl groups on PPh_3 were disordered and refined by using restraints. CCDC 1846846 (**11**), 1846847 (**12**), and 1846845 (**13**) contain the supplementary crystallographic data for this paper. These data can be obtained free of charge from The Cambridge Crystallographic Data Centre.

Crystal data for 11

$[C_{74}H_{65}NO_5OsP_3]Cl \cdot H_2O \cdot O \cdot 2CH_2Cl_2$ ($M = 1538.69$ g mol $^{-1}$): monoclinic; crystal dimensions: $0.40 \times 0.40 \times 0.40$ mm; space group: $P21/c$ (no. 14); $a = 16.5649(4)$, $b = 13.3273(3)$, $c = 32.1022(8)$ Å; $\alpha = 90$, $\beta = 93.801(2)$, $\gamma = 90^\circ$; $V = 7071.5(3)$ Å 3 ; $Z = 4$; $T = 293(2)$ K; $\mu(Mo_{K\alpha}) = 2.111$ mm $^{-1}$; $D_{calcd} = 1.445$ g cm $^{-3}$; 35 339 reflections measured ($6.114^\circ \leq 2\theta \leq 54.998^\circ$); 16 230 unique ($R_{int} = 0.0425$, $R_{sigma} = 0.0639$),

which were used in all calculations. The final R_1 was 0.0552 ($I > 2\sigma(I)$) and wR_2 was 0.1152 (all data); $GOF = 1.116$; residual electron density [e Å $^{-3}$] max min $^{-1}$: 2.36/–3.43.

Crystal data for 12

$[C_{75}H_{59}O_4OsP_3]BF_4 \cdot 0.5CH_2Cl_2$ ($M = 1436.60$ g mol $^{-1}$): triclinic; crystal dimensions: $0.60 \times 0.40 \times 0.40$ mm space group $P-1$ (no. 2); $a = 12.5667(4)$, $b = 13.4395(4)$, $c = 21.4741(4)$ Å; $\alpha = 94.233(3)$, $\beta = 96.881(3)$, $\gamma = 116.602(3)^\circ$; $V = 3186.1(2)$ Å 3 ; $Z = 2$; $T = 293(2)$ K; $\mu(Mo_{K\alpha}) = 2.182$ mm $^{-1}$; $D_{calcd} = 1.497$ g cm $^{-3}$; 26 776 reflections measured ($4.78^\circ \leq 2\theta \leq 54.998^\circ$); 14 633 unique ($R_{int} = 0.0301$, $R_{sigma} = 0.0453$), which were used in all calculations. The final R_1 was 0.0304 ($I > 2\sigma(I)$) and wR_2 was 0.1001 (all data); $GOF = 0.789$; residual electron density [e Å $^{-3}$] max min $^{-1}$: 1.74/–1.47.

Crystal data for 13

$[C_{57}H_{46}O_4OsP_2] \cdot CH_3OH$ ($M = 1079.12$ g mol $^{-1}$): triclinic; crystal dimensions: $0.40 \times 0.40 \times 0.40$ mm; space group $P-1$ (no. 2); $a = 12.5186(5)$, $b = 12.6233(6)$, $c = 15.9741(5)$ Å; $\alpha = 82.613(3)$, $\beta = 86.494(3)$, $\gamma = 71.299(4)^\circ$; $V = 2370.67(17)$ Å 3 ; $Z = 2$; $T = 293(2)$ K; $\mu(Mo_{K\alpha}) = 2.808$ mm $^{-1}$; $D_{calcd} = 1.512$ g cm $^{-3}$; 22 221 reflections measured ($6.248^\circ \leq 2\theta \leq 54.998^\circ$); 10 878 unique ($R_{int} = 0.0283$, $R_{sigma} = 0.0406$), which were used in all calculations. The final R_1 was 0.0260 ($I > 2\sigma(I)$) and wR_2 was 0.0598 (all data); $GOF = 1.058$; residual electron density [e Å $^{-3}$] max min $^{-1}$: 0.94/–1.03.

Computational details

All the optimizations were performed with the Gaussian 09 software package^[25] at the B3LYP level of density functional theory.^[26] Frequency calculations were performed to confirm the characteristics of the calculated structures as minima. In the B3LYP calculations, the effective core potentials (ECPs) of Hay and Wadt with a double- ξ valence basis set (LanL2DZ) were used to describe the Os, P, and Cl atoms, and the standard 6-31G(d) basis set was used for all other atoms.^[27] Polarization functions were added for Os ($\xi(f) = 0.886$), P ($\xi(d) = 0.34$), and Cl ($\xi(d) = 0.514$).^[28]

Acknowledgements

This work was supported by the National Natural Science Foundation of China (No.s.: 21472155, 21772160, 21561162001).

Conflict of interest

The authors declare no conflict of interest.

Keywords: carbolong • metallaaromatics • metallafurans • osmium • reaction mechanism • steric hindrance

- [1] For reviews, see: a) B. J. Frogley, L. J. Wright, *Chem. Eur. J.* **2018**, *24*, 2025–2038; b) B. J. Frogley, L. J. Wright, *Coord. Chem. Rev.* **2014**, *270–271*, 151–166; c) X. Cao, Q. Zhao, Z. Lin, H. Xia, *Acc. Chem. Res.* **2014**, *47*, 341–354; d) C. Zhu, X. Cao, H. Xia, *Chin. J. Org. Chem.* **2013**, *33*, 657; e) A. F. Dalebrook, L. J. Wright, *Adv. Organomet. Chem.* **2012**, *60*, 93–177; f) M. Paneque, M. L. Poveda, N. Rendón, *Eur. J. Inorg. Chem.* **2011**, 19–33; g) J. R. Bleeke, *Acc. Chem. Res.* **2007**, *40*, 1035–1047; h) L. J. Wright, *Dalton Trans.* **2006**, 1821–1827; i) C. W. Landorf, M. M. Haley, *Angew. Chem. Int. Ed.* **2006**, *45*, 3914–3936; *Angew. Chem.* **2006**, *118*,

- 4018–4040; j) G. He, H. Xia, G. Jia, *Chin. Sci. Bull.* **2004**, *49*, 1891–1899; k) J. R. Bleeker, *Chem. Rev.* **2001**, *101*, 1205–1228; l) J. R. Bleeker, *Acc. Chem. Res.* **1991**, *24*, 271–277.
- [2] For examples, see: a) B. J. Frogley, L. C. Perera, L. J. Wright, *Chem. Eur. J.* **2018**, *24*, 4304–4309; b) Y. García-Rodeja, I. Fernández, *Chem. Eur. J.* **2017**, *23*, 6634–6642; c) B. J. Frogley, L. J. Wright, *Angew. Chem. Int. Ed.* **2017**, *56*, 143–147; *Angew. Chem.* **2017**, *129*, 149–153; d) J. Huang, X. Zhou, Q. Zhao, S. Li, H. Xia, *Chin. J. Chem.* **2017**, *35*, 420–428; e) F. Han, J. Li, H. Zhang, T. Wang, Z. Lin, H. Xia, *Chem. Eur. J.* **2015**, *21*, 565–567; f) R. Lin, K. H. Lee, H. H. Y. Sung, I. D. Williams, Z. Lin, G. Jia, *Organometallics* **2015**, *34*, 167–176; g) Á. Vivancos, Y. Hernández, A. M. Paneque, M. L. Poveda, V. Salazar, E. Álvarez, *Organometallics* **2015**, *34*, 177–188; h) F. Han, T. Wang, J. Li, H. Zhang, H. Xia, *Chem. Eur. J.* **2014**, *20*, 4363–4372; i) R. Lin, K. Lee, K. C. Poon, H. H. Y. Sung, I. D. Williams, Z. Lin, G. Jia, *Chem. Eur. J.* **2014**, *20*, 14885–14899; j) Á. Vivancos, M. Paneque, M. L. Poveda, E. Álvarez, *Angew. Chem. Int. Ed.* **2013**, *52*, 10068–10071; *Angew. Chem.* **2013**, *125*, 10252–10255; k) T. Wang, H. Zhang, F. Han, L. Long, Z. Lin, H. Xia, *Chem. Eur. J.* **2013**, *19*, 10982–10991; l) T. Wang, H. Zhang, F. Han, L. Long, Z. Lin, H. Xia, *Angew. Chem. Int. Ed.* **2013**, *52*, 9251–9255; *Angew. Chem.* **2013**, *125*, 9421–9425; m) K. C. Poon, L. Liu, T. Guo, J. Li, H. H. Y. Sung, I. D. Williams, Z. Lin, G. Jia, *Angew. Chem. Int. Ed.* **2010**, *49*, 2759–2762; *Angew. Chem.* **2010**, *122*, 2819–2822; n) G. R. Clark, L. A. Ferguson, A. E. McIntosh, T. Sohnel, L. J. Wright, *J. Am. Chem. Soc.* **2010**, *132*, 13443–13452; o) M. Paneque, C. M. Posadas, M. L. Poveda, N. Rendón, V. Salazar, E. Oñate, C. Mereiter, *J. Am. Chem. Soc.* **2003**, *125*, 9898–9899; p) V. Jacob, T. J. R. Weakley, M. M. Haley, *Angew. Chem. Int. Ed.* **2002**, *41*, 3470–3473; *Angew. Chem.* **2002**, *114*, 3620–3623; q) R. D. Gilbertson, T. J. R. Weakley, M. M. Haley, *Chem. Eur. J.* **2000**, *6*, 437–441; r) R. D. Gilbertson, T. J. R. Weakley, M. M. Haley, *J. Am. Chem. Soc.* **1999**, *121*, 2597–2598; s) G. P. Elliott, W. R. Roper, J. M. Waters, *J. Chem. Soc. Chem. Commun.* **1982**, 811–813.
- [3] For reviews, see: a) G. Jia, *Organometallics* **2013**, *32*, 6852–6866; b) J. Chen, G. He, G. Jia, *Chin. J. Org. Chem.* **2013**, *33*, 792–798; c) J. Chen, G. Jia, *Coord. Chem. Rev.* **2013**, *257*, 2491–2521; d) G. Jia, *Coord. Chem. Rev.* **2007**, *251*, 2167–2187; e) G. Jia, *Acc. Chem. Res.* **2004**, *37*, 479–486.
- [4] See for examples: a) W. Ruan, T.-F. Leung, C. Shi, K. H. Lee, H. H. Y. Sung, I. D. Williams, Z. Lin, G. Jia, *Chem. Sci.* **2018**, *9*, 5994–5998; b) T. B. Wen, K. H. Lee, J. Chen, W. Y. Hung, W. Bai, H. Li, H. H. Y. Sung, I. D. Williams, Z. Lin, G. Jia, *Organometallics* **2016**, *35*, 1514–1525; c) Q. Zhuo, X. Zhou, H. Kang, Z. Chen, Y. Yang, F. Han, H. Zhang, H. Xia, *Organometallics* **2016**, *35*, 1497–1504; d) J. Chen, K. H. Lee, T. B. Wen, F. Gao, H. H. Y. Sung, I. D. Williams, Z. Lin, G. Jia, *Organometallics* **2015**, *34*, 890–896; e) J. Chen, C. Shi, H. H. Y. Sung, I. D. Williams, Z. Lin, G. Jia, *Chem. Eur. J.* **2012**, *18*, 14128–14139; f) J. Chen, C. Shi, H. H. Y. Sung, I. D. Williams, Z. Lin, G. Jia, *Angew. Chem. Int. Ed.* **2011**, *50*, 7295–7299; *Angew. Chem.* **2011**, *123*, 7433–7437; g) J. Chen, H. H. Y. Sung, I. D. Williams, Z. Lin, G. Jia, *Angew. Chem. Int. Ed.* **2011**, *50*, 10675–10678; *Angew. Chem.* **2011**, *123*, 10863–10866; h) W. Y. Hung, B. Liu, W. Shou, T. B. Wen, C. Shi, H. H. Y. Sung, I. D. Williams, Z. Lin, G. Jia, *J. Am. Chem. Soc.* **2011**, *133*, 18350–18360; i) B. Liu, H. Xie, H. Wang, L. Wu, Q. Zhao, J. Chen, T. B. Wen, Z. Cao, H. Xia, *Angew. Chem. Int. Ed.* **2009**, *48*, 5461–5464; *Angew. Chem.* **2009**, *121*, 5569–5572; j) G. He, J. Zhu, W. Y. Hung, T. B. Wen, H. H. Y. Sung, I. D. Williams, Z. Lin, G. Jia, *Angew. Chem. Int. Ed.* **2007**, *46*, 9065–9068; *Angew. Chem.* **2007**, *119*, 9223–9226; k) T. B. Wen, W. Y. Hung, H. H. Y. Sung, I. D. Williams, G. Jia, *J. Am. Chem. Soc.* **2005**, *127*, 2856–2857; l) T. B. Wen, S. M. Ng, W. Y. Hung, Z. Y. Zhou, M. F. Lo, L. Y. Shek, I. D. Williams, Z. Lin, G. Jia, *J. Am. Chem. Soc.* **2003**, *125*, 884–885; m) T. B. Wen, Z. Y. Zhou, G. Jia, *Angew. Chem. Int. Ed.* **2001**, *40*, 1951–1954; *Angew. Chem.* **2001**, *113*, 2005–2008.
- [5] a) R. Grande-Aztatzi, J. M. Mercero, E. Matito, G. Frenking, J. M. Ugalde, *Phys. Chem. Chem. Phys.* **2017**, *19*, 9669–9675; b) K. An, T. Shen, J. Zhu, *Organometallics* **2017**, *36*, 3199–3204; c) J. Chen, K. H. Lee, H. H. Y. Sung, I. D. Williams, Z. Lin, G. Jia, *Angew. Chem. Int. Ed.* **2016**, *55*, 7194–7198; *Angew. Chem.* **2016**, *128*, 7310–7314; d) J. Wei, Y. Zhang, Y. Chi, L. Liu, W. X. Zhang, Z. Xi, *J. Am. Chem. Soc.* **2016**, *138*, 60–63.
- [6] See for examples: a) W. Ma, C. Yu, Y. Chi, T. Chen, L. Wang, J. Yin, B. Wei, L. Xu, W. Zhang, Z. Xi, *Chem. Sci.* **2017**, *8*, 6852–6856; b) Y. Zhang, Y. Chi, J. Wei, Q. Yang, Z. Yang, H. Chen, R. Yang, W. X. Zhang, Z. Xi, *Organometallics* **2017**, *36*, 2982–2986; c) W. Ma, C. Yu, T. Chen, L. Xu, W. Zhang, Z. Xi, *Chem. Soc. Rev.* **2017**, *46*, 1160–1192; d) J. Wei, W. Zhang, Z. Xi, *Angew. Chem. Int. Ed.* **2015**, *54*, 5999–6002; *Angew. Chem.* **2015**, *127*, 6097–6100; e) J. Wei, Y. Zhang, W. Zhang, Z. Xi, *Angew. Chem. Int. Ed.* **2015**, *54*, 9986–9990; *Angew. Chem.* **2015**, *127*, 10124–10128.
- [7] a) F. Feixas, E. Matito, J. Poater, M. Solà, *Chem. Soc. Rev.* **2015**, *44*, 6434–6451; b) I. Fernández, G. Frenking, G. Merino, *Chem. Soc. Rev.* **2015**, *44*, 6452–6463; c) I. Fernández, G. Frenking, *Chem. Eur. J.* **2007**, *13*, 5873–5884; d) D. L. Thorn, R. Hoffmann, *Nouv. J. Chim.* **1979**, *3*, 39–45.
- [8] a) M. Mauksch, S. B. Tsogoeva, *Chem. Eur. J.* **2010**, *16*, 7843–7851; b) H. Hua, H. Zhang, H. Xia, *Chin. J. Org. Chem.* **2018**, *38*, 11–28.
- [9] a) J. Wei, W. X. Zhang, Z. Xi, *Chem. Sci.* **2018**, *9*, 560–568; b) Y. Zhang, J. Wei, Y. Chi, X. Zhang, W. Zhang, Z. Xi, *J. Am. Chem. Soc.* **2017**, *139*, 5039–5042; c) L. Liu, M. Zhu, H. T. Yu, W. Zhang, Z. Xi, *J. Am. Chem. Soc.* **2017**, *139*, 13688–13691.
- [10] a) Q. Zhuo, H. Zhang, Y. Hua, H. Kang, X. Zhou, X. Lin, Z. Chen, J. Lin, K. Zhuo, H. Xia, *Sci. Adv.* **2018**, *4*, eaat0336; b) X. Zhou, Y. Li, Y. Shao, Y. Hua, H. Zhang, Y. Lin, H. Xia, *Organometallics* **2018**, *37*, 1788–1794; c) J. Chen, Q. Lin, S. Li, Z. Lu, J. Lin, Z. Chen, H. Xia, *Organometallics* **2018**, *37*, 618–623; d) Q. Zhuo, J. Lin, Y. Hua, X. Zhou, Y. Shao, S. Chen, Z. Chen, J. Zhu, H. Zhang, H. Xia, *Nat. Commun.* **2017**, *8*, 1912; e) R. Li, Z. Lu, Y. Cai, F. Jiang, C. Tang, Z. Chen, J. Zheng, J. Pi, R. Zhang, J. Liu, Z. Chen, Y. Yang, J. Shi, W. Hong, H. Xia, *J. Am. Chem. Soc.* **2017**, *139*, 14344–14347; f) M. Luo, L. Long, H. Zhang, Y. Yang, Y. Hua, G. Liu, Z. Lin, H. Xia, *J. Am. Chem. Soc.* **2017**, *139*, 1822–1825; g) X. Zhou, J. Wu, Y. Hao, C. Zhu, Q. Zhuo, H. Xia, J. Zhu, *Chem. Eur. J.* **2018**, *24*, 2389–2395; h) C. Zhu, J. Wu, S. Li, Y. Yang, J. Zhu, X. Lu, H. Xia, *Angew. Chem. Int. Ed.* **2017**, *56*, 9067–9071; *Angew. Chem.* **2017**, *129*, 9195–9199; i) C. Zhu, X. Zhou, H. Xing, K. An, J. Zhu, H. Xia, *Angew. Chem. Int. Ed.* **2015**, *54*, 3102–3106; *Angew. Chem.* **2015**, *127*, 3145–3149; j) C. Zhu, Y. Yang, J. Wu, M. Luo, J. Fan, J. Zhu, H. Xia, *Angew. Chem. Int. Ed.* **2015**, *54*, 7189–7192; *Angew. Chem.* **2015**, *127*, 7295–7298; k) Q. Zheng, *Sci. China Chem.* **2014**, *57*, 1059–1060.
- [11] a) C. Zhu, H. Xia, *Acc. Chem. Res.* **2018**, *51*, 1691–1700; b) X. Zhou, J. Wu, Y. Hao, C. Zhu, Q. Zhuo, H. Xia, J. Zhu, *Chem. Eur. J.* **2018**, *24*, 2296; c) S. K. Ritter, *C&EN* **2016**, *94*, 9; d) H. Xia, *Chin. J. Chem.* **2018**, *36*, 78; e) Z. Lu, J. Chen, H. Xia, *Chin. J. Org. Chem.* **2017**, *37*, 1181–1188.
- [12] C. Zhu, M. Luo, Q. Zhu, J. Zhu, P. v. R. Schleyer, J. I. C. Wu, X. Lu, H. Xia, *Nat. Commun.* **2014**, *5*, 3265.
- [13] M. Luo, C. Zhu, L. Chen, H. Zhang, H. Xia, *Chem. Sci.* **2016**, *7*, 1815–1818.
- [14] C. Zhu, Y. Yang, M. Luo, C. Yang, J. Wu, L. Chen, G. Liu, T. B. Wen, J. Zhu, H. Xia, *Angew. Chem. Int. Ed.* **2015**, *54*, 6181–6185; *Angew. Chem.* **2015**, *127*, 6279–6283.
- [15] Z. Lu, C. Zhu, Y. Cai, J. Zhu, Y. Hua, Z. Chen, J. Chen, H. Xia, *Chem. Eur. J.* **2017**, *23*, 6426–6431.
- [16] a) C. Zhu, S. Li, M. Luo, X. Zhou, Y. Niu, M. Lin, J. Zhu, Z. Cao, X. Lu, T. B. Wen, Z. Xie, P. v. R. Schleyer, H. Xia, *Nat. Chem.* **2013**, *5*, 698–703; b) Q. Zhu, C. Zhu, Z. Deng, G. He, J. Chen, J. Zhu, H. Xia, *Chin. J. Chem.* **2017**, *35*, 628–634.
- [17] C. Zhu, Q. Zhu, J. Fan, J. Zhu, X. He, X. Y. Cao, H. Xia, *Angew. Chem. Int. Ed.* **2014**, *53*, 6232–6236; *Angew. Chem.* **2014**, *126*, 6346–6350.
- [18] a) Q. Lin, S. Li, J. Lin, M. Chen, Z. Lu, C. Tang, Z. Chen, X. He, J. Chen, H. Xia, *Chem. Eur. J.* **2018**, *24*, 8375–8381; b) Z. Lu, Y. Cai, Y. Wei, Q. Lin, J. Chen, X. He, S. Li, W. Wu, H. Xia, *Polym. Chem.* **2018**, *9*, 2092–2100; c) X. He, X. He, S. Li, K. Zhuo, W. Qin, S. Dong, J. Chen, L. Ren, G. Liu, H. Xia, *Polym. Chem.* **2017**, *8*, 3674–3678; d) C. Yang, G. Lin, C. Zhu, X. Pang, Y. Zhang, X. Wang, X. Li, B. Wang, H. Xia, G. Liu, *J. Mater. Chem. B* **2018**, *6*, 2528–2535; e) C. Zhu, C. Yang, Y. Wang, G. Lin, Y. Yang, X. Wang, J. Zhu, X. Chen, X. Lu, G. Liu, H. Xia, *Sci. Adv.* **2016**, *2*, e1601031.
- [19] a) H. Wang, X. Zhou, H. Xia, *Chin. J. Chem.* **2018**, *36*, 93–105; b) G. He, J. Chen, H. Xia, *Sci. Bull.* **2016**, *61*, 430–442.
- [20] K. Ouyang, Z. Xi, *Acta Chim. Sinica* **2013**, *71*, 13–25.
- [21] A. Bondi, *J. Phys. Chem.* **1964**, *68*, 441–451.
- [22] O. V. Dolomanov, L. J. Bourhis, R. J. Gildea, J. A. K. Howard, H. Puschmann, *J. Appl. Crystallogr.* **2009**, *42*, 339–341.
- [23] G. M. Sheldrick, *Acta Crystallogr. Sect. A* **2015**, *71*, 3–8.
- [24] G. M. Sheldrick, *Acta Crystallogr. Sect. C* **2015**, *71*, 3–8.
- [25] Gaussian 09, Revision D.01, M. J. Frisch, G. W. Trucks, H. B. Schlegel, G. E. Scuseria, M. A. Robb, J. R. Cheeseman, G. Scalmani, V. Barone, B. Mennucci, G. A. Petersson, H. Nakatsuji, M. Caricato, X. Li, H. P. Hratchian, A. F. Izmaylov, J. Bloino, G. Zheng, J. L. Sonnenberg, M. Hada, M. Ehara, K. Toyota, R. Fukuda, J. Hasegawa, M. Ishida, T. Nakajima, Y. Honda, O. Kitao, H. Nakai, T. Vreven, J. A. Montgomery Jr., J. E. Peralta, F. Ogliaro,

- M. Bearpark, J. J. Heyd, E. Brothers, K. N. Kudin, V. N. Staroverov, R. Kobayashi, J. Normand, K. Raghavachari, A. Rendell, J. C. Burant, S. S. Iyengar, J. Tomasi, M. Cossi, N. Rega, J. M. Millam, M. Klene, J. E. Knox, J. B. Cross, V. Bakken, C. Adamo, J. Jaramillo, R. Gomperts, R. E. Stratmann, O. Yazyev, A. J. Austin, R. Cammi, C. Pomelli, J. W. Ochterski, R. L. Martin, K. Morokuma, V. G. Zakrzewski, G. A. Voth, P. Salvador, J. J. Dannenberg, S. Dapprich, A. D. Daniels, Farkas, J. B. Foresman, J. V. Ortiz, J. Cioslowski, D. J. Fox, Gaussian Inc., Wallingford, CT, **2013**.
- [26] a) A. D. Becke, *J. Chem. Phys.* **1993**, *98*, 5648–5652; b) B. Miehlich, A. Savin, H. Stoll, H. Preuss, *Chem. Phys. Lett.* **1989**, *157*, 200–206; c) C. Lee, W. Yang, R. G. Parr, *Phys. Rev. B.* **1988**, *37*, 785–789.
- [27] P. J. Hay, W. R. Wadt, *J. Chem. Phys.* **1985**, *82*, 299–310.
- [28] *Gaussian Basis Sets for Molecular Calculations*, (Ed.: S. Huzinaga), Elsevier, Amsterdam, **1984**.

Manuscript received: June 7, 2018

Accepted manuscript online: July 16, 2018

Version of record online: September 4, 2018